Quantization of excitons in CuCl epitaxial thin films: Behavior between a two-dimensional quantum well and the bulk

Z. K. Tang,* A. Yanase, and Y. Segawa
Photodynamics Research Center, The Institute of Physical and Chemical Research (RIKEN), Nagamachi Koeji, 19-1399, Aoba-ku, Sendai 980, Japan

N. Matsuura and K. Cho
Faculty of Engineering Science, Osaka University, Toyonaka, Osaka 560, Japan
(Received 19 August 1994)

A study of quantized excitons in CuCl epitaxial thin films is reported. Film thicknesses (L) that are much smaller than the photon wavelength (λ) in the medium (~ 160 nm), but larger than the exciton Bohr radius a_B (~ 0.7 nm), are considered here. Many structures have been observed in transmission and absorption spectra over the Z_3 exciton region. When $L < 30$ nm, these structures correspond well to the confined exciton levels with odd quantum number n. The oscillator strength for the nth quantized exciton is found to be proportional to L/n^2 for odd n and zero for even n. The absence of the states with even n in the optical spectra is interpreted in terms of the parity selection rule in the confined exciton system where the long-wavelength approximation holds. The measured optical spectra are compared with the additional-boundary condition-free response theory. Polariton-interference fringes given by the theory demonstrate a good agreement with the experimental results both for thick and thin films. By analyzing the absorption line shape, the dependence of nonradiative damping of the quantized exciton on quantum number n and film thickness L is discussed.

I. INTRODUCTION

Excited by resonant light, an electron and a hole are created in conduction and valence bands, respectively, forming an exciton. Because of translational symmetry in a bulk crystal, only the exciton having the same wave vector ($\mathbf{K}$) as the photon can be optically created,[1] which is the so-called $\mathbf{K}$ selection rule of the exciton in a bulk crystal. The exciton and photon with the same $\mathbf{K}$ are coupled with each other, forming polaritons. By decreasing the crystal size, the translational crystal symmetry breaks down in the size-reduced direction, and the exciton is confined in this direction. The problem of quantum confinement of the exciton and propagation of the polariton in low-dimensional crystals has attracted much attention both because of the understanding of the fundamental physics of the confined exciton system and the large application potential to nonlinear optical devices.

Many interesting features in the confined exciton system have been expected, which are different from those in bulk crystal. The qualitative behavior of the exciton in the confined exciton system is characterized by several relevant lengths such as Bohr radius a_B of the exciton and the photon wavelength λ in the medium. For a thin crystal with thickness L, when $L \leq a_B$, an electron and a hole are first of all confined separately in the layer direction, leading to discrete subbands both for the electron and the hole. Because of the carrier confinements, the exciton formed from these subbands shows two-dimensional behavior and its binding energy is strongly enhanced. The optical transitions between the valence and conduction subbands obey a selection rule of $\Delta n = n_e - n_h = 0$ with a constant oscillator strength independent on the electron and the hole quantum numbers (n_e, n_h) and the well thickness.[2] The polariton propagation is allowed only in the layer plane. The properties of the exciton in this confinement regime have been extensively studied in quantum-well (QW) structures of III-V compounds both theoretically and experimentally.[2] For an intermediate size of confinement from the QW regime to the bulk, the center-of-mass (c.m.) motion of the exciton is quantized, while the relative motion is essentially identical to that in the bulk crystal except for a possible distortion near the surfaces. The coupling with the light field in this situation can be described as the multiple internal reflection of bulk (upper and lower) polaritons, which leads to interference effects in resonance spectra. The multimode interference of polaritons is equivalent to the exciton c.m. quantization.[3] The positions of resonant structures in optical spectra are shifted from the quantized exciton levels, especially near the bottom of the exciton band. This is due to the multimode interference of polaritons, or equivalently, to the radiative shift of each quantized level. For general thickness, all the quantized levels are optically active, though the intensity changes alternatively with quantum numbers. The polariton-interference structures have been first observed in CdS, CdSe,[4,5] and later in CuCl,[6] CdTe/ZeTe thin films,[7–10] and recently in GaAs thin films.[11–13] These interference structures can be analyzed by solving the Maxwell equations with an additional boundary condition (ABC),[3,4,14] or by an ABC-free theory.[15,16]

When the film thickness is thin enough as compared with the photon wavelength in the medium but still large

enough as compared with the exciton Bohr radius, $a_B \ll L \ll \lambda$, we found that the exciton spectra could be simply interpreted in terms of the concept of *local oscillators* characterized by $\{E_n, f_n\}$ in the long-wavelength approximation (LWA), where E_n and f_n are the resonant energy and the oscillator strength, respectively, of the quantized exciton with quantum number n.[17] Optical transitions from the ground state to such quantized exciton states follow the parity selection rule of the confined exciton wave functions. A brief description of the oscillator strength and the parity selection rule of the exciton in ultrathin CuCl films was given in 17.

Compared to the III-V and II-VI compounds, CuCl has a large binding energy ($\sim$190 meV) and a small Bohr radius ($\sim$0.7 nm) of the exciton. The electron-hole Coulomb interaction will be strong enough to maintain the bulklike electron-hole relative motion, down to a surprisingly small film thickness. The CuCl film system thus appears interesting for studying the c.m. quantization of the exciton state. However, only a few works on the exciton c.m. quantization in the CuCl film system have been reported.[6,18–20]

In the present paper, transmission and absorption spectra are reported for CuCl epitaxial films with various thicknesses. The obtained spectra are compared to the exciton c.m. quantization and the polariton interference. It is found that when $L < 30$ nm, the confined exciton system can be well understood with the parity selection rule of the exciton wave function and the exciton oscillator in the LWA. For thicker samples, the spectral structures become complex, and the parity selection rule breaks down. The oscillator strength and the nonradiative damping factor of the quantized exciton are determined as functions of the film thickness and the quantization number by analyzing the line shape of the absorption spectra.

II. EXPERIMENT

CuCl films used in the measurements were grown on MgO(001) substrates using the molecular-beam-epitaxy technique. The CuCl overlayer with (111) orientation consists of four types of domains with specific crystallographic relationships with respect to the lattice of MgO.[21] An atomic-force-microscope (AFM) topography showed that the size of the domains was about 1 μm, which is larger than those grown on other substrates.[22] Streaked reflection-high-energy-electron-diffraction patterns indicated that the CuCl thin film is relatively flat.[21] The growth rate of CuCl was monitored by a quartz oscillator inside the growth chamber, and the film thickness was obtained by *ex situ* ellipsometric measurements using a 400-nm laser line (double frequency of a Ti:sapphire laser) as a light source and AFM tomograph. The accuracy of the thickness measurement was estimated to be $\pm(1-1.5)$ nm.

Near-normal incident transmission and reflection spectra were measured using a 150-W xenon lamp for the samples immersed in superfluid He ($\sim$2 K). The excitation light was dispersed by a 50-cm single monochromator, and focused onto the sample ($\sim$0.5-mm spot size). The spectral resolution was about 0.2 meV in this optical system. The transmitted and reflected light were detected directly with a GaAs photomultiplier coupled with a lock-in amplifier. Curves (a) and (b) in Fig. 1 show reflection and transmission spectra for the 15.7$\pm$1.5-nm sample at 2 K, respectively. Some clear structures are seen in the spectra, which will be discussed later. The absorption spectrum, as shown by curve (c) in the figure, is obtained from the reflection and transmission spectra: $\alpha L = -\ln(I/I_0^*) = -\ln[T/(1-R)]$, where α is the absorption coefficient, I_0 is the intensity of the incident light, and $I_0^* = I_0(1-R)$ is the intensity of the light propagated in the medium.

III. EXPERIMENTAL RESULTS AND DISCUSSION

A. Exciton confinement and polariton interference in a thin film

Transmission spectra of CuCl thin films are shown in Fig. 2 for samples of $L = 30\pm1$, 48 ± 1, and 54.5 ± 1 nm by curves (a), (b), and (c), respectively. In order to clarify the structures in the resonance region, a logarithmic scale is used for the ordinate in the figure. Several transmission dips are seen over the Z_3 1s-exciton region. As seen from the figure, both relative intensities and energy positions of these structures strongly depend on the film thickness. Energy positions of the polariton (lower-

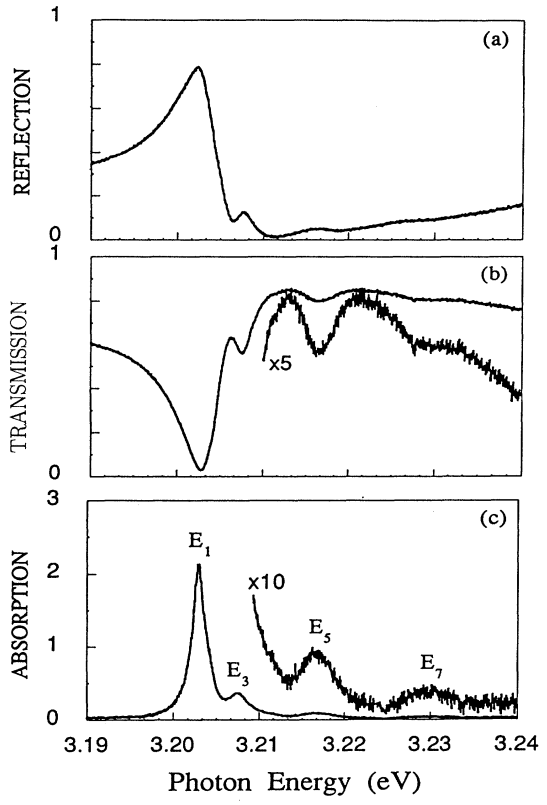

FIG. 1. Reflection (a), transmission (b), and absorption (c) spectra in CuCl thin film of $L = 15.7\pm1.5$ nm at 2 K.

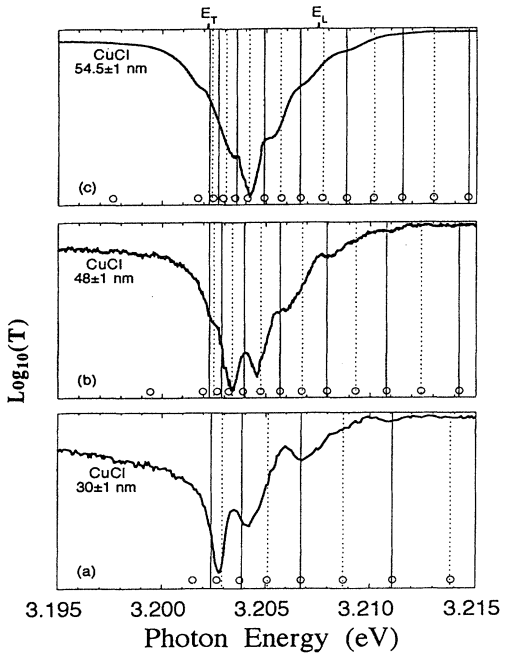

FIG. 2. Transmission spectra of CuCl thin films at 2 K. (a) $L=30\pm1$ nm, (b) $L=48\pm1$ nm, and (c) $L=54.5\pm1$ nm. The ordinate is logarithmic. Energy positions of polariton and exciton for the values of $K_n=n\pi/L$ with $n=1,2,3,\ldots,$ are shown by open circles and vertical lines, respectively.

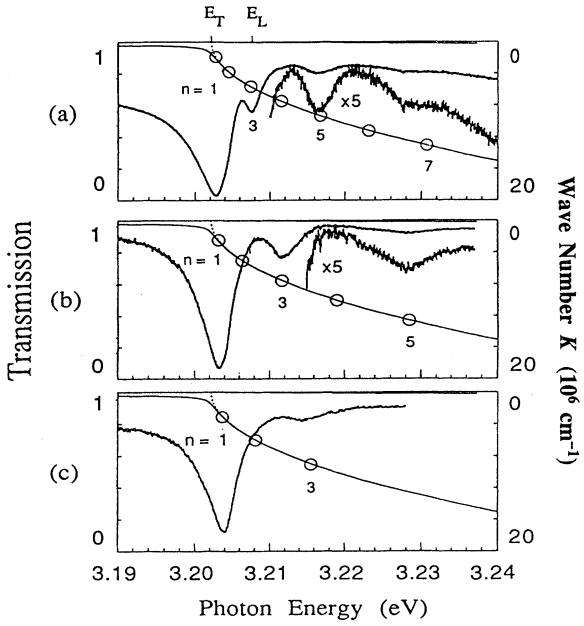

FIG. 3. Transmission spectra of CuCl thin films at 2 K. (a) $L=15.7\pm1.5$ nm, (b) $L=12.4\pm1.5$ nm, and (c) $L=9.7\pm1.5$ nm. Polariton and exciton dispersion are also shown by thin solid lines and dotted lines, respectively. Open circles represent the positions of $K_n=n\pi/L$ with $n=1,2,3,\ldots$.

branch polariton) and exciton for the size-quantized values of translational wave number $K_n=n\pi/L$, ($n=1,2,3,\ldots,$), are also shown in the same figure by open circles and vertical lines, respectively. Clearly, there is no simple correlation between the transmission structures and the energy positions given by K_n in the resonant region (near the bottom of the exciton band). On the high-energy side, the transmission structures almost correspond to the exciton energy with K_n but the spacing is the double of π/L. A similar result has been observed in the CdS and CdSe plates,[4,5] and in CuCl thin crystal.[6] These structures have been interpreted as an effect of interference between the upper polariton (UP) and the lower polariton (LP). More details of this multimode (UP and LP) interference have been discussed by Cho *et al.*[16]

Figure 3 shows spectra for thinner samples of $L=9.7\pm1.5$, 12.4 ± 1.5, and 15.7 ± 1.5 nm. The dotted and thin solid lines shown in the figure are the dispersion curves for the exciton and polariton in a bulk crystal, respectively, and the open circles are their energy positions for the size-quantized values of translational wave number K_n. Some discrete transmission dips are clearly seen. The ratios of their relative intensities seem to be almost constant for different thickness while their amplitudes rapidly decrease with quantum number n. The positions of these dips coincide well with the energy positions of the quantized exciton except for the states of even n, and they shift to the higher-energy side as the film thickness decreases, showing the behavior of the quantum-size effects on excitation energies of excitons.

Many theoretical studies of the optical properties of excitons in thin films have been published.[4,5,15,16,23] D'Andrea and Del Sole[14] have discussed the exciton wave functions confined in a thin film by taking into account a dead layer (or transition layer) near the surface. A "no-escape" boundary condition for the exciton wave function leads to the quantization of the c.m. momentum

$$K_nL=n\pi+2\tan^{-1}(K_n/P),\quad n=1,2,3,\ldots \tag{1}$$

with the dead layer of thickness $1/P$. The exciton energy is then given as a series of discrete levels:

$$E_n=E_T+(\hbar K_n)^2/2M,\quad n=1,2,3,\ldots, \tag{2}$$

where $M=m_e+m_h$ is the exciton translational mass and E_T is the rest energy of the transverse exciton in a bulk crystal. The effect of the dead layer, however, was shown to be negligible in CuCl by the analysis of the extraordinarily fine interference pattern.[3] Thus, Eq. (1) is simply given as $K_n=n\pi/L$ ($n=1,2,3,\ldots,$).

Now we move our attention to the polariton aspects of the thin-film optics and compare the experimental results with a calculation based on the ABC-free theory.[15] In the ABC-free theory, the optical linear susceptibility is given in a nonlocal form as

$$\chi_n(Z,Z',E)=\frac{2}{L}\hbar B\sum_n\frac{\sin(K_nZ)\sin(K_nZ')}{E_n-E-i\Gamma_n}, \tag{3}$$

where B is a constant, which can be estimated from the L-T splitting of the exciton in a bulk crystal, $\sin(K_nZ)$ is

the wave function for the exciton c.m. motion with coordinate Z, and Γ_n is the phenomenologically introduced nonradiative damping factor. By carrying out the summation over all of n in Eq. (3), the optical response has been shown to be equivalent to the interference scheme due to the UP and LP using Pekar's ABC.[3] In Eq. (3), Γ_n is the only unknown parameter that can be determined in such a way that the calculated line shape agrees well with the experimental one. Curves (a)–(d) in Fig. 4 show the calculated results for $L=48\pm1$ nm with various nonradiative damping factors, and curve (e) is the experimental one. When a constant value of $\Gamma_n=0.02$ meV is used, as shown by curves (a), the calculated spectrum is characterized by narrow and sharp structures. Clearly, the constant (energy independent) Γ_n cannot explain the experimental spectra, as in the analysis of the $L=150$-nm sample.[3] Here, we assume an energy-dependent nonradiative damping factor

$$\Gamma_n=\alpha\frac{\Delta E_n}{n}=\alpha\frac{\hbar^2\pi^2}{2M}\left[\frac{n}{L^2}\right], \tag{4}$$

where α is a proportionality constant and $\Delta E_n=E_n-E_T$ is the quantization energy of the exciton. Curves (b), (c), and (d) correspond to $\alpha=0.3$, 0.6, and 0.9, respectively. The spectra are strongly affected by the nonradiative damping factor. A very good agreement between theoretical and experimental spectra is obtained when $\alpha=0.9$. A detailed discussion on the nonradiative damping factor for a quantized exciton will be given in Sec. III D. Figure 5 shows the experimental (exp) spectrum and the theoretical (cal) one, which is calculated with

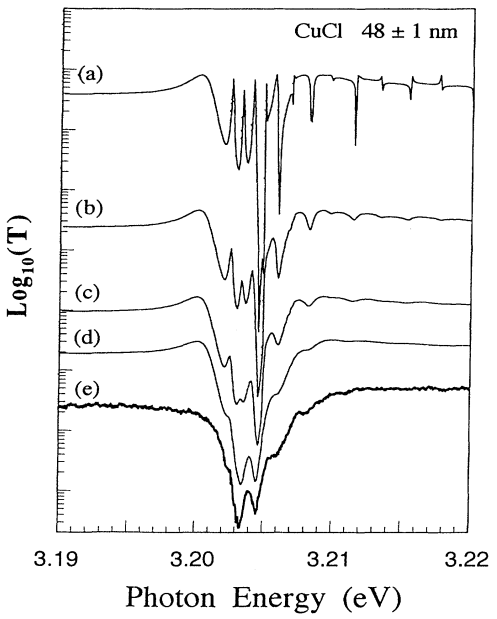

FIG. 4. Calculated transmission spectra, curves (a)–(d), for CuCl thin film of $L=48$ nm using various nonradiative damping. (a) $\Gamma_n=0.02$ meV; (b), (c), and (d) using Γ_n described by Eq. (4) for $\alpha=0.3$, 0.6, and 0.9, respectively. Curve (e) is the experimental spectrum for $L=48\pm1$ nm.

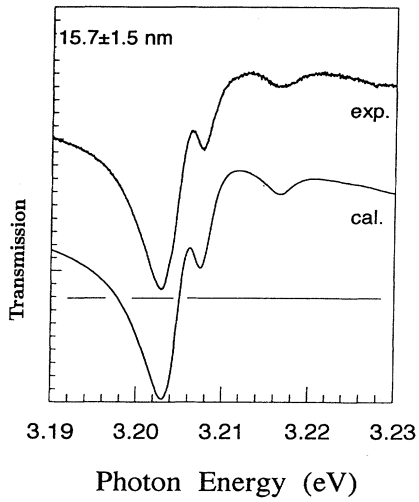

FIG. 5. Experimental (exp) and calculated (cal) transmission spectra of $L=15.7\pm1.5$ nm.

$\alpha=0.9$ for a thinner sample of $L=15.7\pm1$ nm. As seen in the figure, the polariton-interference structure completely coincides with quantized exciton states of odd quantum number even near the bottom of the exciton energy band. The same results are obtained for other samples of $L<30$ nm, which demonstrates the equivalence of exciton quantization and polariton interference. The polariton interference and the exciton quantization are two aspects of the same phenomenon.

B. Optical selection rule of confined excitons in the LWA

In the previous section, it was shown that the alternating strength of the oscillation structures in transmission spectra are well described by the multimode interference of the exciton polariton both for thick and for thin (as shown in Figs. 4 and 5) films. This description, however, has to rely on a tedious calculation even for a qualitative interpretation. In this section, we give a direct and simple description of the optical spectra of a thin film in which the LWA is valid. It is seen in Fig. 3 that the transmission dips correspond quite well to the quantized states with odd quantum number n, while the dip amplitude decreases rapidly with the increase of n. The film thicknesses shown in Fig. 3 are much smaller than the resonant photon wavelength (~160 nm), i.e., LWA ($L\ll\lambda$) holds in these samples. In this case, the spatial variation of the light field in the medium is expected to be negligible. Now we discuss the results shown in Fig. 3 in terms of the c.m. quantization of the exciton in LWA. We assume that only a light wave with a refractive index $n=\sqrt{\epsilon_0}$ is propagating in the medium, where ϵ_0 is the background dielectric constant. This light excites mechanical excitons. The ground state of the crystal is given by

$$\Psi_g=\prod_R \varphi_R^{(v)}, \tag{5}$$

where $\varphi_R^{(v)}$ is the Wannier function of the electron in a valence orbital centered at R. After excitation by the external field, an electron is transferred to the conduction band, leaving a hole in the valence band. An exciton state is a linear combination of electron-hole pair states as

$$\Psi_{\lambda,n}=\sum_{\beta}\sum_{R}F_n(Z)\phi_\lambda(\beta)\left[\varphi_{R+\beta}^{(c)}\prod_{R'\neq R}\varphi_{R'}^{(v)}\right], \tag{6}$$

where $\varphi_{R+\beta}^{(c)}$ is the Wannier function centered at $R+\beta$ of an electron in the conduction band, $F_n(Z)$ and $\phi_\lambda(\beta)$ are the envelope functions describing the c.m. motion of the exciton with quantum number n and the electron-hole relative motion with quantum number λ, respectively, Z is the coordinate of the exciton c.m. motion along the growth direction of the film, and β is the relative distance between the electron and the hole. For bulk crystal, $F_n(Z)$ is a plane wave, and $\phi_\lambda(\beta)$ is a hydrogenlike function.[1] If we neglect the small dead-layer effect on CuCl surfaces,[3] the envelope functions for the c.m. motion are simply given by $F_n(Z)=(2/L)^{1/2}\sin(n\pi Z/L)$, which has even parity for the states of odd n and odd parity for those of even n. The envelope function for the relative motion is essentially identical to that of bulk crystal in this confinement regime. For the $1s$ exciton, $\phi_{1s}(\beta)=(\pi a_B^3)^{-1/2}\exp(-\beta/a_B)$. Thus, the matrix element of the electric dipole operator (P) for the transition between the ground state Ψ_g and excited state $\Psi_{\lambda,n}$ is given, in LWA, by

$$\begin{aligned}\langle\Psi_{\lambda,n}|P|\Psi_g\rangle&=\left[\frac{2}{L}\right]^{1/2}\sum_{R}\sin(K_nZ)\\&\quad\times\sum_{\beta}\phi_\lambda(\beta)\\&\quad\times\langle\varphi_{R+\beta}^{(c)}|P|\varphi_R^{(v)}\rangle|_{\beta=0}\\&=\left[\frac{2}{L}\right]^{1/2}\sum_{R}\sin(K_nZ)\phi_\lambda(0)\\&\quad\times\langle\varphi_R^{(c)}|P|\varphi_R^{(v)}\rangle\ .\end{aligned} \tag{7a}$$

The size dependence of the Wannier function $\varphi_R^{(c,v)}$ is negligible because of its local property. And we can reasonably assume that $\varphi_R^{(c,v)}$ is the same for every atomic position. (Strictly speaking, the φ_R for those atoms on the crystal surface would be different from that of inner atoms.) Therefore, the dipole-transition element $\langle\varphi_R^{(c)}|P|\varphi_R^{(v)}\rangle$ is approximately a constant and can be removed from the summation of Eq. (7a). Hence, Eq. (7a) is simply given by

$$\begin{aligned}\langle\Psi_{\lambda,n}|P|\Psi_g\rangle&=\left[\frac{2}{L}\right]^{1/2}\phi_\lambda(0)\langle\varphi^{(c)}|P|\varphi^{(v)}\rangle\\&\quad\times\int_0^L\sin(K_nZ)dZ\\&=\frac{\sqrt{L}}{n}\{1-(-1)^n\}\frac{\sqrt{2}}{\pi}\phi_\lambda(0)\\&\quad\times\langle\varphi^{(c)}|P|\varphi^{(v)}\rangle\ .\end{aligned} \tag{7b}$$

Here the summation $\sum_R$ over the positions in Eq. (7a) was replaced by the integration over the film thickness L in Eq. (7b). The matrix element has a nonzero value only for odd quantum number n. That is, only those exciton states with odd n contribute to the optical transitions. That is why no structures are observed corresponding to even quantum numbers n in the transmission spectra shown in Fig. 3. Ascribing the observed peaks to odd n's, we made a comparison of exciton energies in Fig. 6. Open circles are the experimental data for the excited states $n=1,3,5,\ldots$, and dotted lines are calculated according to Eq. (2) using $M_T=2.3m_0$ and $E_T=3.2022$ eV,[24] demonstrating a good agreement.

The same selection rule described above has also been theoretically expected in the confined phonon system.[25] Hence, the parity selection rule seems a common property of the confined boson. Because the LWA can hardly be realized in the confined phonon system, it would be difficult to observe the parity selection rule in the experiment in the confined phonon system.

C. Oscillator strength of the quantized excitons

From the viewpoint of the mechanical exciton, one could naively regard the quantized exciton in a thin film as an assembly of local oscillators with their resonant energy E_n and oscillator strength f_n. From the exciton wave function, f_n per unit area can be easily calculated in LWA as[25]

$$f_n=\tfrac{2}{3}\frac{2}{\hbar\omega m_0}|\langle\Psi_{v,n}|P|\Psi_g\rangle|^2\ , \tag{8}$$

where $\frac{2}{3}$ is from the spin-orbit factor of the Z_3 exciton, m_0 is the free-electron mass, and $\hbar\omega$ is the excitonic transition energy. Inserting Eq. (7b) into Eq. (8), we obtain

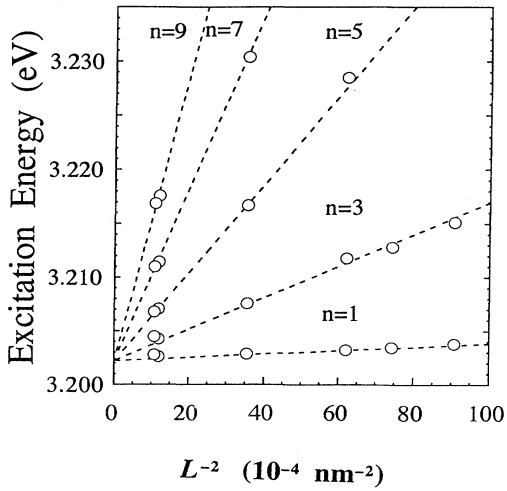

FIG. 6. Quantized exciton energy vs L^{-2} for quantum numbers $n=1,3,\ldots,9$.

$$f_n = \frac{8}{3}\frac{|p_{cv}|^2}{\hbar\omega m_0}|\phi_{1s}(0)|^2\frac{L}{n^2}[1-(-1)^n]^2 . \quad (9)$$

Here $|p_{cv}|^2$ depends on the dipole matrix element between the Wannier functions of the conduction and valence bands, which can be evaluated from the bulk L-T splitting. Expression (9) shows that the oscillator strength of the exciton with resonant energy E_n is proportional to L/n^2 for odd quantum number n and zero for even quantum number n. The zero value of f_n for even n is the result of the parity selection rule of the quantized exciton in LWA. The size (L) enhancement of f_n is due to the coherent extension of the exciton wave function over the whole thickness.[26] But it should be noted that the saturation of radiative width for $n=1$ ($\propto f_1$) starts to appear already at $L\sim\lambda/10\approx 16$ nm (Ref. 27) (see also Fig. 9). The behavior of the oscillator strength given by Eq. (9) is completely different from that in a QW where the oscillator strength per unit area depends neither on the quantum number of the electron and hole nor the film thickness.[2]

Now we compare the experimental results with the theoretical expectation. To obtain the oscillator strengths for the respective quantized excitons, we show the absorption spectra in Fig. 7 for the samples of $L=15.7\pm1.5$, 12.4 ± 1.5, and 9.7 ± 1.5 nm, respectively, by curves (a), (b), and (c). The absorption bands E_1, E_3, E_5, and E_7 are well separated in the figure. They correspond to the exciton levels of $n=1$, 3, 5, and 7, respectively. The oscillator strengths, f_n, per unit area for the respective exciton states are then obtained from the integration of these separate absorption bands and are plotted in Fig. 8 as functions of n^2. Solid circles, squares, and open circles shown in Fig. 8 are for the samples of $L=15.7\pm1.5$, 12.4 ± 1.5, and 9.7 ± 1.5 nm, respectively. The dotted lines (a), (b), and (c) are calculated according to Eq. (9) for the thicknesses in the same order. As seen from the figure, f_n increases almost linearly with film thickness, but decreases with n^{-2}, in accordance with the theoretical expectation.

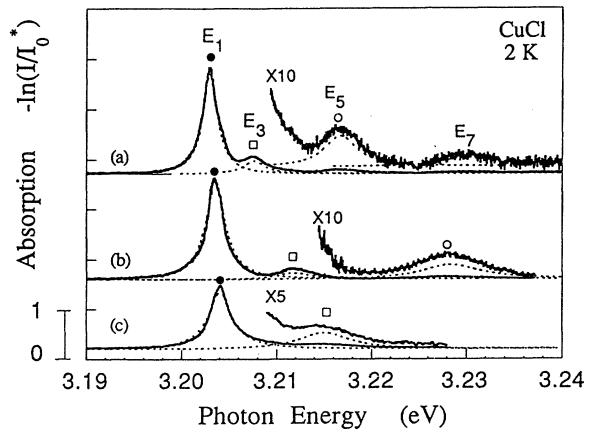

FIG. 7. Absorption spectra of CuCl films with thicknesses (a) 15.7 ± 1.5 nm, (b) 12.4 ± 1.5 nm, and (c) 9.7 ± 1.5 nm at 2 K. Absorption bands are separated by dotted curves.

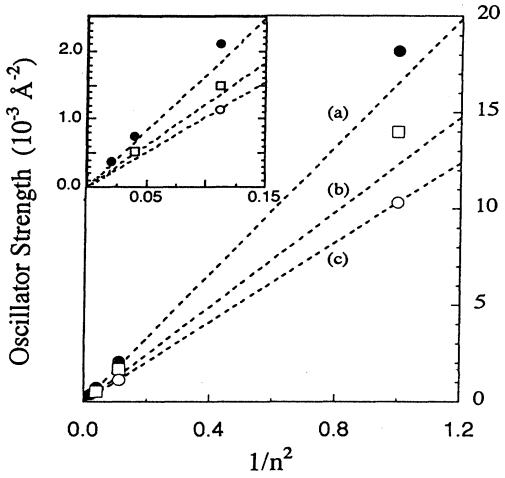

FIG. 8. Oscillator strength plotted against n^{-2}. Dotted lines (a), (b), and (c) are the calculations for $L=15.7$, 12.4, and 9.7 nm, respectively.

D. Spectral width of the quantized exciton

Each resonant structure contains information about the radiative and nonradiative damping. If we denote the corresponding widths as D and F, respectively, the peak width in the absorption spectrum $A=(1-T-R)$ is shown to be the sum of D and F.[27] In the LWA, D is proportional to the oscillator strength of the peak. Thus, the result of Sec. II C shows that D is proportional to the system size L in the LWA. The L dependence of D can be calculated also beyond the LWA by using the ABC-free, or nonlocal response theory, which allows us to derive F from the comparison with the present measurement.

In both the local and nonlocal response theories, the equation to determine the (linear) response of matter to incident light can be written in the matrix form as

$$[S]\{X\}=\{C\} , \quad (10)$$

which corresponds to solving Schrödinger and Maxwell equations self-consistently within the linear-response regime. Here $\{X\}$ and $\{C\}$ are related to the response and incident field amplitudes, respectively. In the local theory, this is the set of equations corresponding to all the Maxwell boundary conditions for a given frequency ω. In the nonlocal theory, it corresponds to the equation for the expansion coefficients of the response field.[15]

The condition for the existence of a finite solution in the absence of the incident light can be written as $\det[S]=0$. This equation is satisfied generally by complex frequencies $\{\omega=\omega_n+i\gamma_n;\ n=1,2,3,\ldots,\}$. The real and imaginary parts (ω_n and γ_n) correspond to the central position and width, respectively, of the nth resonant structure of the optical spectrum. The application of this formalism (for nonlocal response) to a two-level atom in vacuum gives $\gamma=(2/3)\mu^2(\omega/c)^3$, where μ is the transition dipole moment between the two levels. Since this is the same result as in the nonrelativistic QED, the

complex ω's obtained from $\det[S]=0$ are generally expected to give the radiative correction correctly. The same procedure for the local theory should also give the radiative shift and width within the local approximation of susceptibility,[31] since both schemes solve Schrödinger and Maxwell equations self-consistently (with or without local approximation in the treatment of susceptibility).

Applying this (nonlocal) formalism to the present system of a CuCl slab, we obtain γ_n ($n=1,3,5$) as functions of L for a vanishing value of F, as shown in Fig. 9. The use of a finite value of F (as the broadening factor in the linear susceptibility) gives a uniform upward shift to each curve by that amount. This result contains not only the LWA behavior (linear increase with L), but also the saturation effect beyond LWA. It is also confirmed that these widths agree well with those of the calculated absorption $(1-R-T)$, as they should. Using Fig. 9 and the measured values of total width $D+F$, we can determine the n and L dependences of F as in Fig. 10. It can be clearly seen that F is proportional to L^{-2} and n.

There are two different origins for a finite F. The first (F_1) is the one due to the elastic and inelastic scatterings of excitons in a perfect slab. The second (F_2) is the inhomogeneity in the slab thickness for the samples used in this study. Since a slab consists of clusters of about 1 μm diameter for a sample of given thickness as seen from AFM observation,[17] we should expect the inhomogeneity in the thickness.

At present we cannot divide F in Fig. 10 into F_1 and F_2. If a sample of very uniform thickness is available, it should lead to $F=F_1$. Then, we could derive the n and L dependence of F_2. Or, if we have a good theory for F_1, it would lead to dividing F into F_1 and F_2. A principal origin of F_1 may be the inelastic scattering between the confined exciton and acoustic phonon. The exciton coupling to the acoustic phonon is expected to be enhanced in confined exciton systems, due to the decrease of the spatial extent of the exciton with decreasing crystal size.[28] A detailed calculation indicates that the acoustic-phonon scattering vs the deformation potential would lead to the L^{-2}-dependent nonradiative damping factor in quantum-well structures.[29] Because of the contribution of F_2, we could not conclude that acoustic phonons are the main contributions to quantum-confined exciton linewidths, although Fig. 10 showed the same L^{-2} dependence of the spectral widths. A naive argument for F_2 may be given as follows. If δL is the fluctuation of L, the exciton energy would have the fluctuation $\delta E=(\hbar^2\pi^2\delta L/M)(n^2/L^3)$. This should be the contribution of F_2 in the observed spectrum. The n and L dependence of this mechanism alone does not explain those of Fig. 10. However, the n and L dependence of F caused by the inhomogeneity in the slab thickness may not be so straightforward because the energy fluctuation would lead to a change in the elastic scattering of the exciton, which also contributes to F.

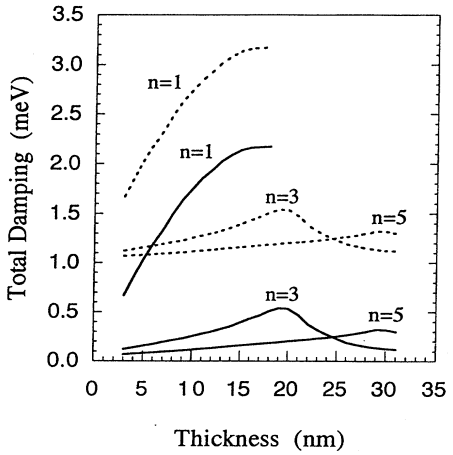

FIG. 9. Calculated total damping (radiative and nonradiative) of the quantized excitons with quantum number $n=1$, 3, and 5 for nonradiative damping 0.05 (solid curves) and 1 meV (dotted curves), respectively.

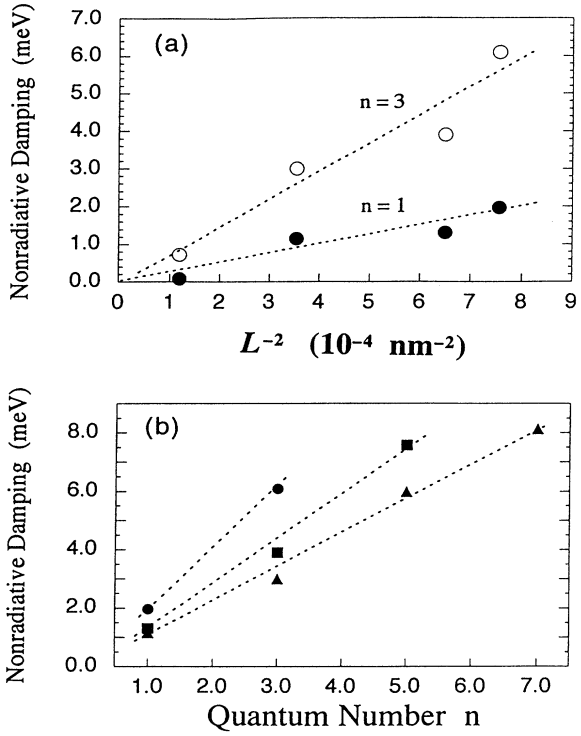

FIG. 10. (a) Nonradiative damping as a function of film thickness L for the $n=1$ and 3 excitons. The dotted curve is calculated in proportion to L^{-2}; (b) as a function of the exciton quantum number n. The circles, squares, and triangles of the data correspond to the samples with $L=9.7\pm1.5$, 12.4 ± 1.5, and 15.7 ± 1.5 nm, respectively.

IV. CONCLUDING REMARKS

We have measured transmission and reflection spectra for CuCl films with various thicknesses. Many structures were seen in the spectra, which were compared with the calculation based on the ABC-free theory developed by Cho.[15] As a polariton system, the spectral shape can be

well interpreted in terms of the polariton interference. This is all right even for very thin films ($L \leq 30$ nm) in which the polariton effect is expected to be less obvious. Due to the presence of multiple branches of the polariton, the spectra show a complex behavior for thick samples in the bottleneck energy region. There is no clear correspondence between the structures of optical spectra and the energies of excitons and polaritons for the values of a quantized wave number because of the existence of an evanescent wave of UP near the bottom of the exciton band (Fig. 2). In the high-energy region, the interference between two propagating waves (UP and LP) leads to the alternating strength of the oscillation structures. In a very thin film, however, the polariton-interference structures coincide well, even near the bottom of the exciton band, with the exciton energies given by quantized wave numbers with odd n (see Figs. 3 and 4). In this situation, an absorption peak corresponds to polariton waves containing large amplitudes of a quantized exciton state, and the radiative shift is much smaller than the level spacing of excitons. But as L increases, the radiative shift and width increase, while the exciton level spacing decreases, so that the absorption peaks are overlapping and become difficult to be mutually distinguished. When the LWA ($L \ll \lambda$) holds, the confinement of the exciton c.m. motion gives another simple and clear interpretation for the observed optical spectra besides the concept of the polariton interference. From the viewpoint of the exciton confinement, the quantized exciton could be regarded as a mechanical oscillator with its resonant energy E_n and oscillator strength f_n. Thus, the alternating intensity of the oscillation structures were explained by the parity selection rule of such a quantized exciton, and their relative intensity was described by f_n. The confined exciton system behaves just like an assembly of local oscillators characterized by $\{E_n, f_n\}$. The damping factors of these oscillators were found to be proportional to n/L^2.

It is worth stressing that the polariton interference in a thin film and the local oscillator of the quantized exciton are two aspects of the same phenomenon. The description of the polariton interference is valid for any film thickness, from a semi-infinite slab to a very thin film so long as the exciton c.m. quantization is a valid approximation. This description, however, is mathematically somewhat tedious, not giving directly the energy position and the relative intensity for optical spectral structures. On the other hand, the description of exciton c.m. confinement by $\{E_n, f_n\}$ gives a very clear physical meaning for the spectral structures. However, it is valid only in the condition of LWA ($L \ll \lambda$) and ceases to yield a quantitative representation of the optical response for thicker films.[3] The condition of the LWA seems very strict because that deviation from the LWA has been seen in the samples of $L \geq 30$ nm (Fig. 2), although the film thickness is still much smaller than the resonant wavelength in the medium (~ 160 nm). For a small value of nonradiative damping, the spatial variation of the internal field shows the breakdown of the LWA even for $L = 28$ nm.[30] If the value of the nonradiative damping factor is very large, it also affects the condition of the LWA. Thus, without knowing this condition, one had better use the nonlocal description.[18,19,24]

ACKNOWLEDGMENTS

We would like to thank Professor T. Goto, Professor T. Itoh, Dr. H. Ishihara, Dr. T. Takagahara, and Professor Y. Kayanuma for their helpful discussions. Z.K.T. and A.Y. wish to acknowledge the support from the Special Researchers' Basic Science Program, RIKEN. This work was partially supported by a Grant-in-Aid for Scientific Research by the Ministry of Education, Science and Culture of Japan.

*Present address: Department of Physics, Hong Kong University of Science and Technology, Clear Water Bay, Kowloon, Hong Kong.

[1]See, for example, Robert S. Knox, *Theory of Excitons* (Academic, New York, 1963).

[2]A collection of relevant reviews can be found in *Excitons in Confined Systems,* edited by R. Del Sole, A. D'Andrea, and A. Lapiccirella (Springer-Verlag, Berlin, 1988); S. Schmitt-Rink, D. S. Chemla, and D. A. B. Miller, Adv. Phys. **38**, 89 (1989).

[3]K. Cho and M. Kawata, J. Phys. Soc. Jpn. **54**, 4431 (1985).

[4]V. A. Kiselev, B. S. Razbirin, and I. N. Uraltsev, Phys. Status Solidi B **72**, 161 (1975).

[5]I. V. Makarenko, I. N. Uraltsev, and V. A. Kiselev, Phys. Status Solidi B **98**, 773 (1980).

[6]T. Mita and N. Nagasawa, Solid State Commun. **44**, 1003 (1982).

[7]H. Tuffigo, R. T. Cox, N. Magnea, Y. Merle D'Aubigne, and A. Million, Phys. Rev. B **37**, 4310 (1988).

[8]H. Tuffigo, B. Lavigen, R. T. Cox, G. Lentz, N. Magnea, and H. Mariette, Surf. Sci. **229**, 480 (1990).

[9]H. Tuffigo, R. T. Cox. G. Lentz, N. Magnea, and H. Mariette, J. Cryst. Growth **101**, 650 (1990).

[10]H. Tuffigo, R. T. Cox, G. Lentz, N. Magnea, and H. Mariette, J. Cryst. Growth **101**, 778 (1990).

[11]J. Kusano, Y. Segawa, M. Mihara, Y. Aoyagi, and S. Namba, Solid State Commun. **72**, 215 (1989).

[12]A. Tredicucci, Y. Chen, F. Bassani, J. Massies, C. Deparis, and G. Neu, Phys. Rev. B **47**, 10 348 (1993).

[13]J. Kusano, Gerrit E. W. Bauer, and Y. Aoyagi, J. Appl. Phys. **75**, 289 (1994).

[14]A. D'Andrea and R. Del Sole, Phys. Rev. B **25**, 3714 (1982).

[15]K. Cho, J. Phys. Soc. Jpn. **55**, 4113 (1986).

[16]K. Cho, A. D'Andrea, R. Del Sole, and H. Ishihara, J. Phys. Soc. Jpn. **59**, 1853 (1990).

[17]Z. K. Tang, A. Yanase, T. Yasui, Y. Segawa, and K. Cho, Phys. Rev. Lett. **71**, 1431 (1993).

[18]Z. K. Tang, A. Yanase, T. Yaui, and Y. Segawa, J. Lumin. **58**, 138 (1994).

[19]Z. K. Tang, A. Yanase, T. Yaui, and Y. Segawa, J. Lumin. **61**,

316 (1994).
[20]D. K. Shuh, R. S. Williams, Y. Segawa, J. Kusano, Y. Aoyagi, and S. Namba, Phys. Rev. B **44**, 5827 (1991).
[21]A. Yanase, Y. Segawa, M. Mihara, M. William Tong, and R. S. Williams, Surf. Sci. Lett. **278**, L105 (1992).
[22]W. M. Tong, E. J. Snyder, R. S. Williams, A. Yanase, Y. Segawa, and M. S. Anderson, Surf. Sci. Lett. **277**, L63 (1992).
[23]A. D'Andrea and R. Del Sole, Phys. Rev. B **41**, 1413 (1990).
[24]W. E. Jones and Ronald Fuchs, Phys. Rev. B **4**, 3581 (1971).
[25]L. C. Andreani, A. D'Andrea, and R. Del Sole, Phys. Lett. A **168**, 451 (1992).
[26]E. Hanamura, Phys. Rev. B **37**, 1273 (1988).
[27]K. Cho, H. Ishihara, and T. Okada, in *Optics of Excitons in Confined Systems,* edited by A. D'Andrea, R. Del Sole, R. Gislanda, and A. Quattropani, IOP Conf. Proc. No. 123 (The Institute of Physics and Physical Society, London, 1992), p. 17.
[28]S. Schmitt-Rink, D. A. B. Miller, and D. S. Chemla, Phys. Rev. B **35**, 8113 (1987).
[29]T. Takagahara, Phys. Rev. B **31**, 6552 (1985).
[30]H. Ishihara and K. Cho, Phys. Rev. B **48**, 7690 (1993).
[31]K. Odani, Y. Ohfuti, and K. Cho, Solid State Commun. **87**, 507 (1993).